This article has been accepted for publication in a future issue of this journal, but has not been fully edited. Content may change prior to final publication. Citation information: DOI 10.1109/ACCESS.2020.3039857, IEEE Access

IEEE Access
Multidisciplinary | Rapid Review | Open Access Journal

Date of publication xxxx 00, 0000, date of current version xxxx 00, 0000.

Digital Object Identifier 10.1109/ACCESS.2020.Doi Number

Improving Velocity of Stick-Slip Piezoelectric Actuators with Optimized Flexure Hinges Based on SIMP Method

Shitong Yang[1], Xiao Xia[1], Xia Liu[2], Guangda Qiao[1], Xiaosong Zhang[1], and Xiaohui Lu[1]

[1]School of Mechatronic Engineeringv, Changchun University of Technology, Changchun 130012, China.
[2]School of Mechanical and vehicle Engineering, Changchun University, Changchun 130022, China.

Corresponding author: luxh13@ccut.edu.cn.

This work was funded by the Project of Industrial Technology Research and Development of Jilin Province Development and Reform Commission (Grant No. 2019C037-6), the Science and Technology Development Plan of Jilin Province (Grant Nos. 20190201108JC and 20200201057JC), and the Technology Research Planning Project of Education Department of Jilin Province (Grant No. JJKH20191293KJ).

ABSTRACT Flexure hinges have been widely applied in driving mechanisms to achieve the high velocity of stick-slip piezoelectric actuators. However, the majority of driving mechanisms are designed with existing flexure hinge forms, and it is difficult for the actuators to realize the optimal velocity performance. Therefore, a systematic method based on the topology optimization to design flexure hinges of driving mechanisms is proposed in this paper for improving the velocity of the actuators. According to the working principle, the velocity can be increased by maximizing displacement of a driving foot along the positive direction of *x*-axis. The optimization problem of flexure hinges is described utilizing the Solid Isotropic Material with Penalization (SIMP) method. To illustrate the proposed method in detail, a four-bar mechanism with optimized flexure hinges is designed. Among them, three optimization schemes are implemented based on positions of flexure hinge design domains, and then deformations and equivalent stresses of the four-bar mechanism are investigated by simulation to find optimal flexure hinge forms. To prove the feasibility of the proposed method, the characteristic experiments of prototype are conducted. When the driving voltage and driving frequency of prototype are 100 $V_{p\text{-}p}$ and 470 Hz, the maximum velocity is 17.50 mm/s, the maximum load is 220 g. And it is interesting to find that the prototype has no backward motion. Compared with the previously reported actuators with four-bar mechanisms, the velocity of prototype is significantly improved.

INDEX TERMS stick-slip piezoelectric actuators, flexure hinges, driving mechanisms, SIMP method, velocity performance.

I. INTRODUCTION

Stick-slip piezoelectric actuators have merits of a high accuracy, rapid response and simpler mechanical structure [1-3], which have attracted extensive attention for scanning probe microscopes, optical focusing, precision machining, micromanipulators, robots and micro/nano mechanical tests [4-11]. The large motion stroke of the actuators is realized by displacement accumulations of a slider (or a rotor), and each displacement consists of a static friction stage and relative sliding stage between the slider and the stator [12,13]. Therefore, the actuators have a characteristic of theoretically unlimited resolution [14]. However, there are challenges in other characteristics of the actuators, these mainly include output velocities, load capacities, etc.

As a driving part of stick-slip piezoelectric actuators, driving mechanisms are the key factor affecting performances. Therefore, driving mechanisms are designed to improve performances of the actuators, especially in terms of the velocity. For example, Li et al. designed a parallelogram flexure hinge mechanism, an equilateral triangle flexure mechanism, and an asymmetrical trapezoid flexure mechanism, respectively [15-17]. Cheng et al. proposed a trapezoid-type right circular flexure hinge mechanism, a mechanism with asymmetrical right-circle flexure hinges and a triangular displacement amplification mechanism with asymmetric flexure hinges, respectively [18-20]. Guo et al. developed a mechanism of asymmetric structure with circular flexure hinges and leaf flexure hinges [21]. From the above research, it can be found that flexure hinges exist in these mechanisms, and their forms

This work is licensed under a Creative Commons Attribution 4.0 License. For more information, see https://creativecommons.org/licenses/by/4.0/

This article has been accepted for publication in a future issue of this journal, but has not been fully edited. Content may change prior to final publication. Citation information: DOI 10.1109/ACCESS.2020.3039857, IEEE Access

and positions have an important influence on the performance of the actuators.

In general, when the driving mechanism of stick-slip piezoelectric actuators is designed, the whole structure of the mechanism is designed, while flexure hinges in the mechanism are designed with existing forms (such as circular flexure hinges and leaf flexure hinges) based on a certain experience [22-25]. This flexure hinge design method will not make flexure hinges play the optimal function in the velocity of the actuators. Therefore, a systematic method needs to be explored to design optimal flexure hinge forms of the driving mechanism to improve the velocity of the actuators.

With the progress of science and technology, the topology optimization has developed rapidly and becomes an increasingly popular tool in the conceptual phase of the design process [26,27]. The topology optimization can find the optimal distribution of materials in the fixed design domain so as to maximize or minimize the design objective while satisfying a series of constraints. Theoretical researches of the topology optimization can go back to the truss theory [28]. Subsequently, various methods of the topology optimization were developed, such as the homogenization method [29], level set method [30], and solid isotropic material with penalization (SIMP) method [31-34]. Among them, the SIMP method replaces the structural material with the imaginary material whose density varies between 0 and 1, and the density is used as a design variable to achieve material reduction. Due to the simple mathematical model and high computational efficiency, the SIMP method has becoming more and more popular and it was widely used in optimization software [35]. Compliant mechanisms have been designed by SIMP method [36,37], so flexure hinges can also be designed by treating them as compliant mechanisms. To improve the velocity of stick-slip piezoelectric actuators, a systematic flexure hinge design method based on the topology optimization is innovatively proposed in this paper.

In the rest of this paper, the optimization objective is determined according to the working principle of flexure hinges stick-slip piezoelectric actuators. Then, a four-bar mechanism with optimized flexure hinges is designed to introduce the proposed method in detail. Finally, to prove the feasibility of the proposed method, the characteristic experiments of prototype are conducted.

II. WORKING PRINCIPLE

The working principle of flexure hinge stick-slip piezoelectric actuators is shown in figure 1. Generally speaking, the sawtooth wave is applied as the driving signal to drive the actuators, and the motion process of the actuators in one cycle can be separated into the following three stages.

Initial stage: Because the piezoelectric stack is not excited by the driving signal when time $t = t_0$, it will not deform. At this time, the driving foot of driving mechanisms is directly contact with the slider in the effect of the maximum static friction force.

Stick stage: From time t_0 to t_1, the piezoelectric stack is excited by the driving signal to extend slowly, which can cause driving mechanisms to produce deformations. The driving foot of driving mechanisms generates a movement due to the stiffness and rotation accuracy of flexure hinges. Under the action of static friction force, the slider can be driven by the driving foot to move a displacement S_1 along the positive direction of x-axis.

Slip stage: From time t_1 to t_2, the piezoelectric stack recovers rapidly. At this time, driving mechanisms will return to its original state. Due to the effect of kinetic friction force and inertia, the slider can move a short displacement S_2 along the negative direction of x-axis.

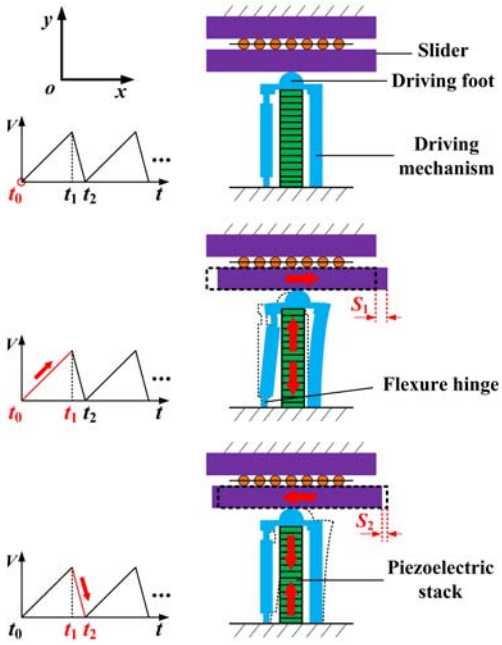

FIGURE 1. The working principle of flexure hinge stick-slip piezoelectric actuators.

After these three stages, a single-step displacement S_d (S_d=S_1-S_2) is produced. Repeating these three stages continuously, the actuators can achieve a large-stroke motion. Moreover, the relationship between the velocity and the single-step displacement can be expressed as:

$$v = f \times S_d \tag{1}$$

In equation (1), v and f represent the velocity and the driving frequency. The velocity v is proportional to the single-step displacement S_d when the driving frequency f is constant. Therefore, the velocity of the actuators can be improved by increasing S_d. Since S_1 has the greatest impact on S_d in one work cycle of the actuators, the single-step displacement S_d can be increased by maximizing the displacement S_1. At the same time, the displacement S_1 of the slider is produced by the driving foot in the action of static friction. Therefore, the velocity of the actuators can be improved by maximizing the displacement S_1 of the driving foot.

This work is licensed under a Creative Commons Attribution 4.0 License. For more information, see https://creativecommons.org/licenses/by/4.0/

This article has been accepted for publication in a future issue of this journal, but has not been fully edited. Content may change prior to final publication. Citation information: DOI 10.1109/ACCESS.2020.3039857, IEEE Access

III. FLEXURE HINGE DESIGN METHOD

To improve the velocity of stick-slip piezoelectric actuators, flexure hinges are designed by proposed method based on the topology optimization. The method includes the optimization problem description, topology optimization of flexure hinges and mechanism design and simulation analysis.

A. OPTIMIZATION PROBLEM DESCRIPTION

The optimization problem of flexure hinges is described employing SIMP method as follows:

$$\begin{aligned} &\text{find}: \boldsymbol{\rho} = (\rho_1, \rho_2, \rho_3, \ldots, \rho_N)^T \in R^N \\ &\max\left\{U_{out}^x = \mathbf{L}_x^T \mathbf{u}\right\} \\ &\text{s. t.}: \mathbf{K}(\boldsymbol{\rho})\mathbf{u} = \mathbf{f} \\ &\quad \frac{\sum_{i=1}^{N} v_i \rho_i}{V} \le V_f \\ &\quad 0 < V_f < 1 \\ &\quad 0 < \rho_{\min} \le \rho_i \le 1, \quad i = 1, \ldots, N \end{aligned} \tag{2}$$

Here ρ_i is the design variable which refers to the material density of each element after the design domain is discretized into a large number of elements. Output displacement U_{out}^x is the objective function representing the displacement S_1 of the driving foot, $\mathbf{u}$ is the displacement vector, $\mathbf{L}_x$ is an adjoint vector representing the load, the inner product of $\mathbf{L}_x$ and $\mathbf{u}$ produces U_{out}^x. $\mathbf{K}$ is the stiffness matrix, $\mathbf{f}$ is the load vector, V is the volume of design domains, v_i is the volume of element i, V_f is the volume fraction. $\rho_{\min}$ is the minimum value of ρ_i.

Since the performance (such as stiffness and rotation accuracy) of flexure hinges is determined by the shape of cross section [37], the volume of flexure hinges is directly related to the performance of flexure hinges when the material and the thickness are the identical. So, the volume fraction is used as the constraint in optimization problem.

B. TOPOLOGY OPTIMIZATION OF FLEXURE HINGES

According to the optimization problem, the topology optimization of flexure hinges is achieved by using the Optistruct solver in Altair HyperMesh [35]. The optimization process is shown in figure 2 and its detailed description is as follows.

As shown in figure 3, in order to introduce the topology optimization process in detail, a simple four-bar mechanism with a semicircular driving foot (the radius is 2.5mm) is selected to execute the topology optimization. The 2D model of the four-bar mechanism is built in figure 4 (a). Among them, four design domains of flexure hinges are divided, and the design domains are arranged in order of 1, 2, 3 and 4. Four design domains have the same size, the length and width are 3.0 mm and 2.5 mm, respectively. Furthermore, except the four design domains, the other domains of the four-bar mechanism are the rigid domain (non-design domain).

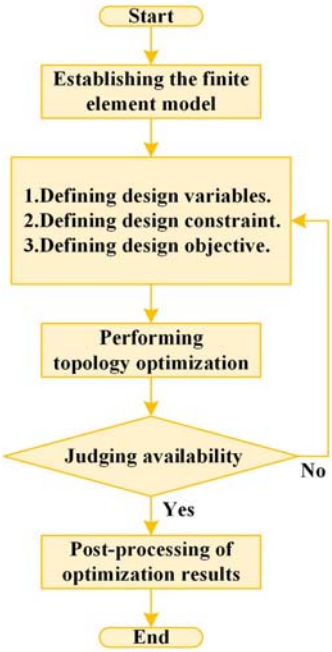

FIGURE 2. Topology optimization process.

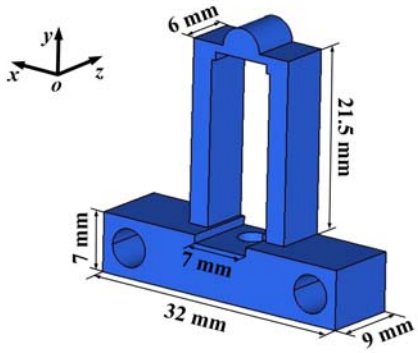

FIGURE 3. A simple four-bar mechanism with a semicircular driving foot

The 2D finite element model is established in figure 4 (b). The meshing is executed in Altair HyperMesh, where have 31099 quadrilateral shell elements with a size of 0.1 mm and 32038 nodes, and each design domain has 750 shell elements. At the same time, two fixing holes are constrained, and the input displacement of 10 μm is imposed. Then, the material is defined, which is aluminium alloy AL7075. Density, Young's modulus, and Poisson's ratio are 2810 kg/m^3, 7.17 × 10^4 MPa, and 0.33, respectively.

After the finite element model is established, the element density (ρ_i) of four design domains is defined as design variables, and the design constraint is the volume fraction (V_f). The design objective is maximum displacement of the top node in the positive direction of x-axis in figure 4 (b). Furthermore, according to different positions of the four design domains, three optimization schemes are proposed as follows.

Scheme I: Four design domains are analyzed one by one.

This work is licensed under a Creative Commons Attribution 4.0 License. For more information, see https://creativecommons.org/licenses/by/4.0/

This article has been accepted for publication in a future issue of this journal, but has not been fully edited. Content may change prior to final publication. Citation information: DOI 10.1109/ACCESS.2020.3039857, IEEE Access

Firstly, performing the topology optimization on design domain 1. Secondly, a flexure hinge is designed based on its optimization result. Then step through the above steps for design domains 2, 3, and 4.

Scheme II: Two design domains are analyzed together. Firstly, performing the topology optimization on design domain 1 and design domain 2. Secondly, two flexure hinges are designed based on their optimization result. Then, the topology optimization is performed on design domain 3 and design domain 4, and two flexure hinges are designed based on their optimization results.

Scheme III: Four design domains are analyzed together. The topology optimization is performed on all design domains. Then, four flexure hinges are designed based on their optimization results.

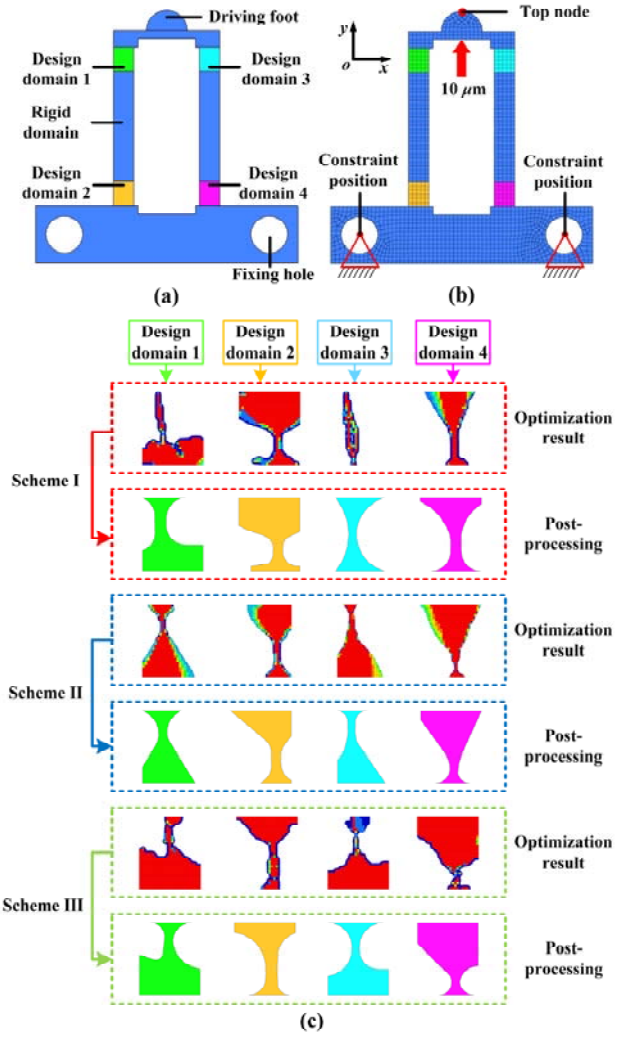

FIGURE 4. The topology optimization of flexure hinges. (a) The 2D model of four-bar mechanism and the design domains of flexure hinges. (b) The 2D finite element model. (c) Optimization result and post-processing.

When the results of topology optimization are generated, the availability of the results is judged by the equivalent stress, and the equivalent stress needs to meet the value allowed by the material of the aluminium alloy AL7075. Otherwise, performing re-optimization by adjusting the volume fraction. Moreover, the iterations of topology optimization in three schemes are given in table I.

TABLE I
ITERATIONS OF TOPOLOGY OPTIMIZATION

Data	Design domain 1	Design domain 2	Design domain 3	Design domain 4
Iterations of scheme I	19	10	19	11
Iterations of scheme II	8	8	12	12
Iterations of scheme III	30	30	30	30

According to the shape of cross section of optimization results in figure 4 (c), the optimization results of design domain 1 and design domain 3 in scheme I have less stiffness, and the optimization results of other design domains have better rotation accuracy. The optimization results of four design domains in scheme II have a well stiffness and rotation accuracy. In scheme III, although the optimization results of four design domains have a certain rotation accuracy, their stiffness is greater. In addition, the optimization process is at conceptual stage in the structural design process, so the optimization results need to be regularization design by post-processing. Based on manufacturing requirement, the post-processing of optimization results in three schemes is performed.

C. MECHANISM DESIGN AND SIMULATION ANALYSIS

In figure 5, in order to find optimal flexure hinge forms from three schemes, three four-bar mechanisms with optimized flexure hinges are devised and the simulation analysis is implemented in HyperMesh. In the simulation analysis, two fixing holes are constrained, and the input of 10 μm is respectively applied under the driving foot of the mechanisms along the positive direction of y-axis. Three mechanisms are shown in figure 5 (a), (b) and (c), whose flexure hinges are designed by scheme I, II and III, respectively. And the deformation of three mechanisms is magnified by the same multiple.

From the simulation analysis, the displacement of driving foot and the equivalent stress in three four-bar mechanisms show a good linear growing with increase of input displacement in figure 6. U_{I}, U_{II} and U_{III} are the displacement of driving foot in the positive x-axis in three mechanisms which are designed based on scheme I, II and III, respectively. The value of U_{I}, U_{II} and U_{III} are 65 μm, 84 μm and 40 μm under the input of 10 μm. Moreover, E_{I}, E_{II} and E_{III} are equivalent stress corresponding to three mechanisms. The value of E_{I}, E_{II} and E_{III} are 98 MPa, 94 MPa and 104 MPa, which are all within the allowable range of aluminium alloy AL7075. It can be seen that the U_{II} is largest in the displacement of these three mechanisms. Therefore, optimal flexure hinge forms are found, and they are obtained based on scheme II.

This work is licensed under a Creative Commons Attribution 4.0 License. For more information, see https://creativecommons.org/licenses/by/4.0/

This article has been accepted for publication in a future issue of this journal, but has not been fully edited. Content may change prior to final publication. Citation information: DOI 10.1109/ACCESS.2020.3039857, IEEE Access

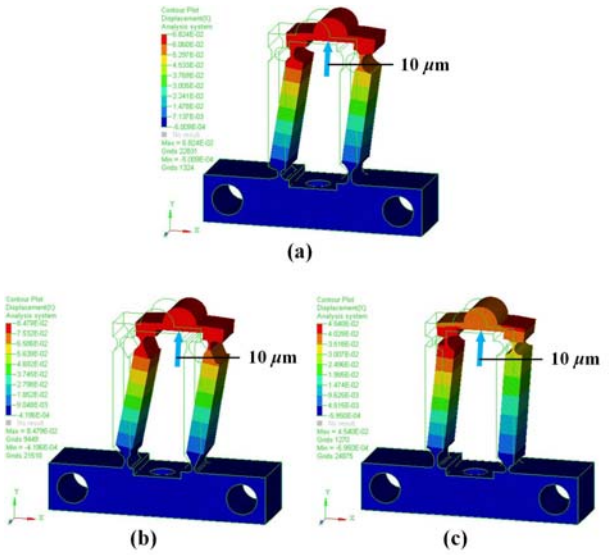

FIGURE 5. The simulation analysis of three four-bar mechanisms designed based on three schemes. (a) Scheme Ⅰ. (b) Scheme Ⅱ. (c) Scheme Ⅲ.

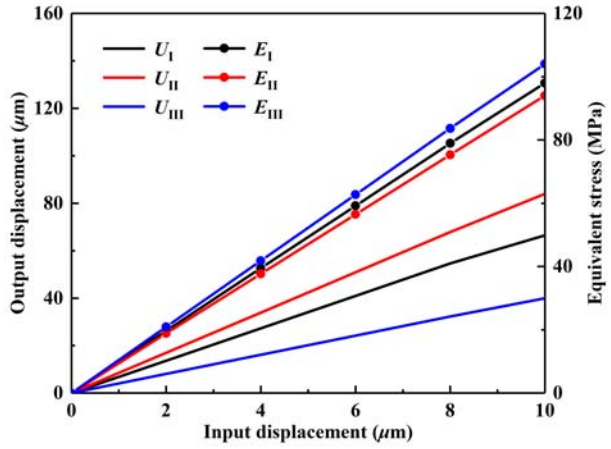

FIGURE 6. The displacement of driving foot and equivalent stress in three four-bar mechanisms.

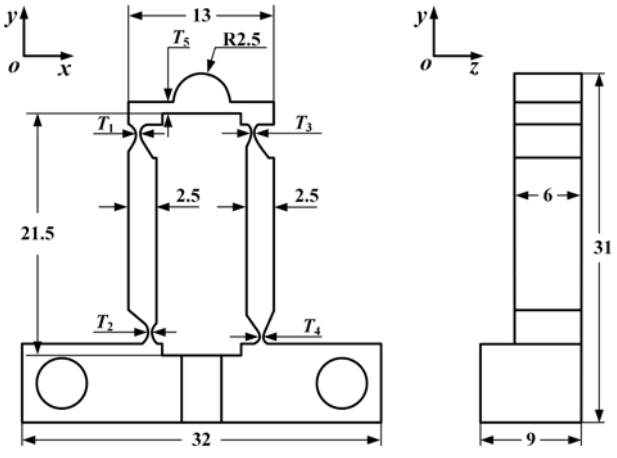

FIGURE 7. The four-bar mechanism with optimal flexure hinge forms and its dimensions (unit: mm).

As shown in figure 7, the four-bar mechanism with optimal flexure hinge forms and its dimensions are revealed. The radius R of the semicircular driving foot is 2.5 mm, and the minimum thickness T_1, T_2, T_3 and T_4 of four flexure hinges are 0.5, 0.5, 0.3 and 0.3 mm, respectively. The dimension of these four flexure hinges is built according to its optimization results, and the smallest size is limited by the machining accuracy, so it is set to 0.3mm. Furthermore, the thickness T_5 of the bar with the driving foot is 1 mm.

VI. EXPERIMENTS

To validate the proposed method, a prototype of actuator with optimal flexure hinge forms is manufactured, and the characteristic experiments of prototype are executed in the experimental system.

A. PROTOTYPE AND EXPERIMENTAL SYSTEM

In figure 8, the prototype with optimal flexure hinge forms is composed of a slider, a base, a stator and an adjusting stage. Among them, the stator contains a driving mechanism, a shim block, a preload screw and a piezoelectric stack. The piezoelectric stack is assembled to the mechanism by applying the shim block and the preload screw. The locking force can be adjusted by the adjusting stage, and it is the maximum static friction force between the driving foot and the slider.

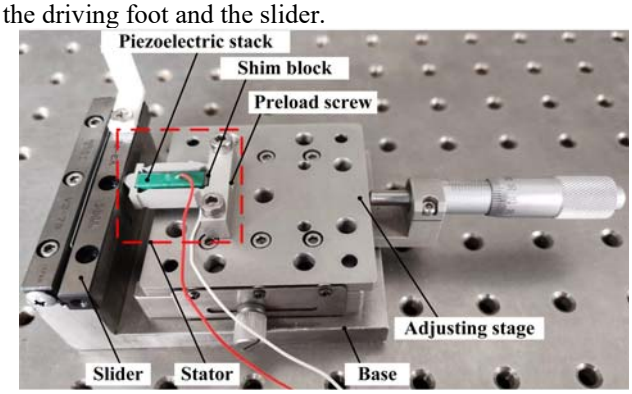

FIGURE 8. Prototype of the actuator with optimal flexure hinges.

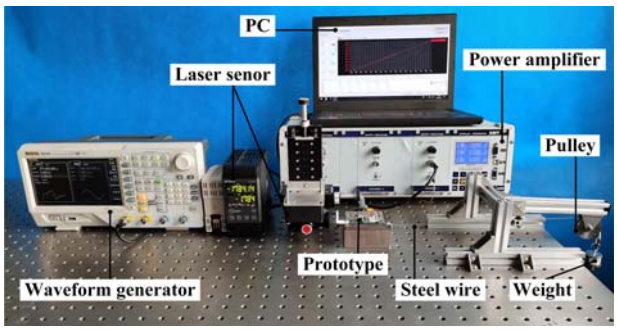

FIGURE 9. Experimental system of the prototype.

Figure 9 shows an experimental system of the prototype. The power amplifier (XE500-C, China) is employed to enlarge the exciting signal which is produced by the waveform generator (DG4162, China). A piezoelectric stack (AE0505D16) with the dimension of 5 mm × 5 mm × 20 mm is formed via NEC-Tokin. The piezoelectric stack produces the deformation under the excitation of the signal, resulting

This work is licensed under a Creative Commons Attribution 4.0 License. For more information, see https://creativecommons.org/licenses/by/4.0/

This article has been accepted for publication in a future issue of this journal, but has not been fully edited. Content may change prior to final publication. Citation information: DOI 10.1109/ACCESS.2020.3039857, IEEE Access

in the continuous output motion of prototype. The stator of prototype pushes the slider which links standard weights by a steel wire and pulley. The mass of the standard weights is identical with the locking force, and it can be adjusted by the adjusting stage. The motion of the slider is gauged by a laser sensor (LK-H020, Japan) with a resolution of 20 nm, the measurement results are received by computer (PC).

B. EXPERIMENTAL RESULTS

When the locking forces of prototype are different, the connection between the velocity and the driving frequency is emerged in figure 10. The velocity rises with growing of the driving frequency when the driving voltage is 100 V_{p-p}. This trend peaks at the driving frequency of 470 Hz, then it decreases. When the locking forces are 1 N, 2 N and 3 N, the maximum velocities of prototype are 17.50 mm/s, 16.97 mm/s and 15.44 mm/s under the driving frequency of 470 Hz.

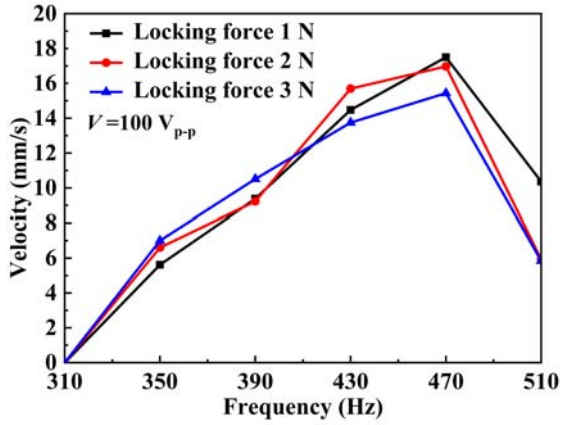

FIGURE 10. Connection between the velocity and the driving frequency.

There is the linear connection between the velocity and the driving voltage of prototype in figure 11. When the locking forces are 1 N, 2 N and 3 N, the velocity grows with the driving voltage gradually increasing under the driving frequency of 470 Hz.

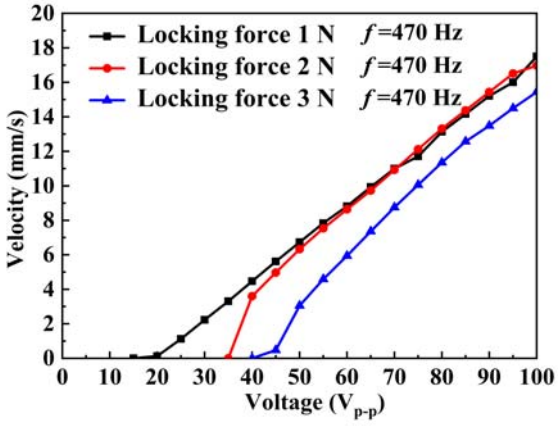

FIGURE 11. Connection between the velocity and the driving voltage.

The connection between the displacement and the time of the slider is demonstrated in figure 12 under the different locking forces. The prototype has a stable operation in every step of stick and slip stage. At the same time, it is interesting to find that the prototype has no backward motion. Figure 13 shows the connection between the velocity and the load. The load of prototype is measured by the standard weight, and the velocity reduces while the load going up. The maximum loads are 160 g, 190 g, 220 g under the locking forces of 1 N, 2 N, 3 N, respectively.

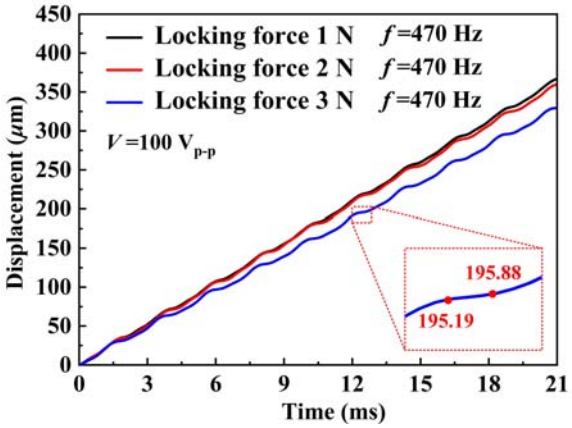

FIGURE 12. Connection between the displacement and the time of the slider.

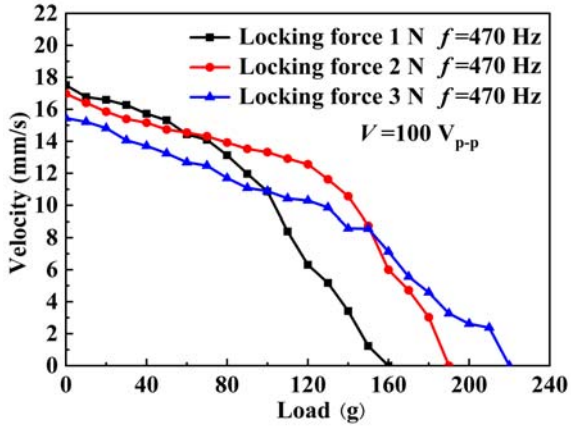

FIGURE 13. Connection between the velocity and the load.

When the locking force and driving frequency of the prototype are 1 N and 470 Hz, the minimum driving voltage is 19.2 V_{p-p}. From the figure 14, the resolution of the prototype reached 83 nm at this point.

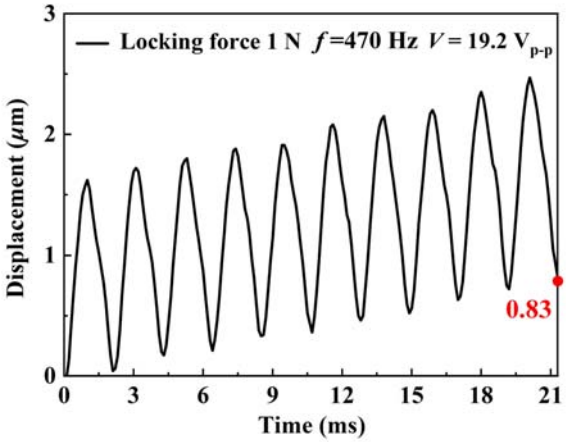

FIGURE 14. Resolution of the prototype under locking force of 1 N.

This work is licensed under a Creative Commons Attribution 4.0 License. For more information, see https://creativecommons.org/licenses/by/4.0/

This article has been accepted for publication in a future issue of this journal, but has not been fully edited. Content may change prior to final publication. Citation information: DOI 10.1109/ACCESS.2020.3039857, IEEE Access

The performance between the prototype and the previously reported actuator with four-bar mechanisms is compared in table II. The maximum velocity of the prototype is higher than the previously reported actuator with four-bar mechanisms. The phenomenon is consistent with the purpose of proposed flexure hinge design method, so the feasibility of the method is verified. Additionally, the velocity and the load of the prototype is better than the previously reported actuator with four-bar mechanisms under the locking force of 2 N. It is shows that the overall performance of the prototype is also excellent.

TABLE II
PERFORMANCE COMPARISON BETWEEN THE PROTOTYPE AND THE PREVIOUSLY REPORTED ACTUATOR WITH FOUR-BAR MECHANISMS.

Actuator	Voltage (V_{p-p})	Frequency (Hz)	Maximum velocity (mm/s)	Velocity under 2N locking force (mm/s)	Load under 2N locking force (g)
[20]	100	500	5.96	5.4	160
[21]	100	490	15.04	11.75	160
Prototype	100	470	17.50	16.97	190

V. CONCLUTION

In this paper, a systematic design method based on the topology optimization was proposed to design optimal flexure hinge forms for improving the velocity of stick-slip piezoelectric actuators. The displacement of the driving foot in the positive direction of *x*-axis was maximized based on the working principle. The optimization problem of flexure hinges was formulated using the SIMP method. Then, a four-bar mechanism with optimized flexure hinges was designed to illustrate the design process. Three optimization schemes were executed according to the position of flexure hinge design domains, and the deformation and equivalent stress were investigated by simulation analysis to find optimal flexure hinge forms. To test the performance of actuator with optimal flexure hinge forms, the characteristic experiments of prototype were implemented. From the experiment results, the maximum velocity and maximum load of the prototype are 17.50 mm/s and 220 g when the driving voltage and driving frequency are 100 V_{p-p} and 470 Hz, respectively. The resolution of the prototype achieves 83 nm. And there is no backward motion during the slip stage of the prototype. Compared with the previously reported actuator with four-bar mechanisms, the velocity of prototype with optimized flexure hinges was improved. It indicated that the proposed systematic design method was feasible, and the method can provide some reference in the further design of flexure hinge stick-slip piezoelectric actuators.

REFERENCES

[1] P. R. Ouyang, R. C. Tjiptoprodjo, W. J. Zhang, G. S. Yang, "Micro-motion devices technology: The state of arts review," *Int. J. Adv. Manuf. Technol.*, vol. 38, pp. 463-478, Aug. 2008.
[2] T. Morita, "Miniature piezoelectric motors," *Sens. Actuat. A- Phys.*, vol. 103, no. 3, pp. 291-300, Feb. 2003.
[3] K. Uchino, "Piezoelectric actuator renaissance," *Phase Trans.*, vol. 88, no. 3, pp. 342-355, Jan. 2015.
[4] V. Cherepanov, P. Coenen, B. Voigtländer, "A nano-positioner for scanning probe microscopy: The KoalaDrive," *Rev. Sci. Instrum.*, vol. 83, no. 2, Feb. 2012, Art. no. 023703.
[5] Y. X. Liu, L. Wang, Z. Z. Gu, Q. Quan and J Deng, "Development of a two-dimensional linear piezoelectric stepping platform using longitudinal-bending hybrid actuators," *IEEE Trans. Ind. Electron.*, vol. 66, no. 4, pp. 3030-3040, Apr. 2019.
[6] Y. Tian, D. Zhang, B. Shirinzadeh, "Dynamic modelling of a flexure-based mechanism for ultra-precision grinding operation," *Precis. Eng.*, vol. 35, no. 4, pp. 554-565, Mar. 2011.
[7] B. E. Kratochvil, L. X. Dong, B. J. Nelson, "Real-time rigid-body visual tracking in a scanning electron microscope," *Int. J. Robo. Res.*, vol. 28, no. 4, pp. 498-511, Apr. 2009.
[8] Y. J. Lin, Z. Chen and B. Yao, "Decoupled torque control of series elastic actuator with adaptive robust compensation of time-varying load-side dynamics," *IEEE Trans. Ind. Electron.*, vol. 67, no. 7, pp. 5604-5614, July. 2020.
[9] J. F. Liao, Z. Chen and B. Yao, "Model-Based coordinated control of four-wheel independently driven skid steer mobile robot with wheel/ground interaction and wheel dynamics," *IEEE Trans. Ind. Inform.*, vol. 15, no. 3, pp. 1742-1752, Mar. 2019.
[10] Y. X. Liu, W. S. Chen, X. H. Yang and J. K. Liu, "A rotary piezoelectric actuator using the third and fourth bending vibration modes," *IEEE Trans. Ind. Electron.*, vol. 61, no. 8, pp. 4366-4373, Aug. 2014.
[11] Y. X Liu, X. H. Yang, W. S. Chen and D. M. Xu, "A bonded-type piezoelectric actuator using the first and second bending vibration modes," *IEEE Trans. Ind. Electron.*, vol. 63, no. 3, pp. 1676-1683, Mar. 2016.
[12] M. Hunstig, T. Hemsel, W. Sextro, "Stick-slip and slip-slip operation of piezoelectric inertia drive—Part I: Ideal excitation," *Sens. Actuat. A-phys.*, vol. 200, pp. 90-100, Oct. 2013.
[13] M. Hunstig, T. Hemsel, W. Sextro, "Stick-slip and slip-slip operation of piezoelectric inertia drive—Part II: Frequency-limited excitation," *Sens. Actuat. A-phys.*, vol. 200, pp. 79-89, Oct. 2013.
[14] M. Hunstig, "Piezoelectric inertia motors-a critical review of history, concepts, design, applications, and perspectives," *Actuators*, vol. 200, pp. 90-100, Oct. 2013.
[15] J. P. Li, J. J. Cai, J. M. Wen, Y. Zhang and N. Wan, "A parasitic type piezoelectric actuator with the asymmetrical trapezoid flexure mechanism," *Sensor. Actuat. A-Phys.*, vol. 309, July. 2020, Art. No. 111907.
[16] J. P. Li, X. Q. Zhou, H. W. Zhao, M. K. Shao, P. L. Hou and X. Q. Xu, "Design and experimental performances of a piezoelectric linear actuator by means of lateral motion," *Smart Mater. Struct.*, vol. 24, no. 6, May. 2015, Art. no. 065007.
[17] J. P. Li, S. C. Chen, G. Zhao, J. M. Wen and N. Wan, "A linear piezoelectric actuator with the parasitic motion of equilateral triangle flexure mechanism," *Smart Mater. Struct.*, vol. 29, no. 1, Nov. 2019, Art. no. 015015.
[18] T. H. Cheng, M. He, H. Y. Li, X. H. Lu, H. W. Zhao and H. B. Gao, "A novel trapezoid-type stick–slip piezoelectric linear actuator using right circular flexure hinge mechanism," *IEEE Trans. Ind. Electron.*, vol. 64, no. 7, pp. 5545-5552, July. 2017.
[19] Q. Gao, M. He, X. H. Lu, C. Zhang and T. H. Cheng, "Simple and high-performance stick-slip piezoelectric actuator based on an asymmetrical flexure hinge driving mechanism," *J. Intell. Mater. Syst Struct.*, vol. 30, no. 14, pp. 2125-2134, July. 2019.
[20] X. H. Lu, Q. Gao, Y. K. Li, Y. Yu, X. S. Zhang, G. D. Qiao, and T. H. Cheng, "A linear piezoelectric stick-slip actuator via triangular displacement amplification mechanism," *IEEE Access*, vol. 8, pp. 6515-6522, Jan. 2020.
[21] Z. Guo, Y. Tian, D. Zhang, T. Wang, M. Wu, "A novel stick-slip based linear actuator using bi-directional motion of micropositioner,"

This work is licensed under a Creative Commons Attribution 4.0 License. For more information, see https://creativecommons.org/licenses/by/4.0/

This article has been accepted for publication in a future issue of this journal, but has not been fully edited. Content may change prior to final publication. Citation information: DOI 10.1109/ACCESS.2020.3039857, IEEE Access

Mech. Syst. Signal. Pr., vol. 128, pp. 37-49, Aug. 2019.

[22] H. Huang, H. W. Zhao, Z. J. Yang, J. Mi, Z. Q. Fan, S. G. Wan, C. L. Shi, and Z. C. Ma, "A novel driving principle by means of the parasitic motion of the microgripper and its preliminary application in the design of the linear actuator," *Rev. Sci. Instrum.*, vol. 83, May. 2012, Art. no. 055002.

[23] Y. K. Zhang, M. L. Wang, Y. M. Fan, T-F. Lu, Y. Cheng, Y. X. Peng, "Improving load capacity of stick-slip actuators in both driving directions via a shared driving foot," *Smart Mater. Struct*., vol. 28, no. 6, May. 2019, Art. no. 065004.

[24] Y. K. Zhang, Y. X. Peng, Z. X. Sun, H. Y. Yu, "A Novel Stick–Slip Piezoelectric Actuator Based on a Triangular Compliant Driving Mechanism," *IEEE Trans. Ind. Electron.*, vol. 66, no. 7, pp. 5374-5382, July. 2019.

[25] Z. Li, L. Zhao and X. Z. Yu, "A novel stick-slip piezoelectric actuator based on two-stage flexible hinge structure," *Rev. Sci. Instrum.*, vol. 91, May. 2020, Art. no. 054704.

[26] E. C. N. Silva, G. Nader, A. B. Shirahige, and J. C. Adamowski, "Characterization of novel flextensional actuators designed by using topology optimization method," *J. Intell. Mater. Syst. Struct.*, vol. 14, nos. 4-5, pp. 297-308, Apr. 2003.

[27] G. K. Lau, H. Du, N. Guo, and M. K. Lim, "Systematic design of displacement-amplifying mechanisms for piezoelectric stacked actuators using topology optimization," *J. Intell. Mater. Syst. Struct.*, vol. 11, no. 9, pp. 685-695, Sep. 2000.

[28] M. I. Frecker, G. K. Ananthasuresh, S. Nishiwaki, N. Kikuchi, S. Kota, "Topological Synthesis of Compliant Mechanisms Using Multi-Criteria Optimization," *J. Mech. Des.*, vol. 119, no. 2, pp. 238-245, Jun. 1997.

[29] P. B. Martin, N. Kikuchi, "Generating optimal topologies in structural design using a homogenization method," *Comput. Methods Appl. Mech. Eng.*, vol. 71, no. 2, pp. 197-224, Mar. 1998.

[30] M. Y. Wang, X. M. Wang, D. M. Guo, "A level set method for structural topology optimization," *Comput. Methods Appl. Mech. Eng.*, vol. 192, nos. 1-2, pp. 227-246, Jan. 2003.

[31] O. Sigmund, "On the design of compliant mechanisms using topology optimization," *Mech. Struct. Mach.*, vol. 25, pp. 493-524, Apr. 1997.

[32] U. D. Larsen, O. Sigmund, S. Bouwstra, "Design and fabrication of compliant micromechanisms and structures with negative poisson's ratio," *J. Microelectromech. S.*, vol. 6, no. 2, pp. 99-106, Jun. 1997.

[33] D. Tcherniak, "Topology optimization of resonating structures using SIMP method," *Int. J. Numer. Meth. Engng.*, vol. 54, no. 11, pp. 1605-1622, May. 2002.

[34] H. Q. Long, Y. M. Hu, X. Q. Jin, H. L. Yu, H. Zhu, "An optimization procedure for spot-welded structures based on SIMP method," *Comp. Mater. Sci.*, vol. 117, pp. 602-607, May. 2016.

[35] B. X. Du, W. Yao, Y. Zhao, X. Q. Chen, "A moving morphable voids approach for topology optimization with closed b-splines," *J. Mech. Des.*, vol. 141, no. 8, Aug. 2019, Art. no. 081401.

[36] S. Canfield and M. Frecker, "Topology optimization of compliant mechanical amplifiers for piezoelectric actuators," *Struct. Multidiscip. O.*, vol. 20, pp. 269-279, Dec. 2000.

[37] M. Liu, X. M. Zhang, and S. Fatikow, "Design and analysis of a high-accuracy flexure hinge," *Rev. Sci. Instrum.*, vol. 87, May. 2016, Art. no. 055106.

This work is licensed under a Creative Commons Attribution 4.0 License. For more information, see https://creativecommons.org/licenses/by/4.0/

This article has been accepted for publication in a future issue of this journal, but has not been fully edited. Content may change prior to final publication. Citation information: DOI 10.1109/ACCESS.2020.3039857, IEEE Access

SHITONG YANG was born in Hebei, majored in mathematics and applied mathematics and received the B.S. degree from Hebei North University, in 2007. He achieved the M.S. degree in applied mathematics from the Northeast Dianli University, in 2011, and the Ph.D. degree in engineering mathematics from Jilin University, in 2014. His research interests include structural optimization, finite element analysis, piezoelectric actuators, and triboelectric nanogenerators.

XIAO XIA was born in 1994 Shandong province, majored in automobile service engineering and received the B.S. degree from ShanDong JiaoTong University, in 2016. He is currently working toward Master of Science in Engineering degree at the Department of Vehicle Engineering from the Changchun University of Technology. His research interests include structural optimization, piezoelectric actuators and triboelectric nanogenerators.

XIA LIU was born in Jilin, China. She received the B.S. degree in mechanical engineering and automation from the Changchun University, Changchun, China, in 2011, the M.S. degree in mechanical engineering from the Changchun University of Technology, Changchun, China, in 2016, now she is working toward doctor degree at Changchun University of Science and Technology, Changchun, China. Her research interests are piezoelectric actuators, and triboelectric nanogenerators.

GUANGDA QIAO was born in Shandong province, China, in 1997. He received the B.S. degree from the Changchun University of Technology, Changchun, China, in 2019. He continues pursuing a Master of Engineering degree in the same school. His research interests include piezoelectric actuators and triboelectric nanogenerators.

XIAOSONG ZHANG was born in Sichuan province, China, in 1996. He received the B.S. degree in mechanical engineering and automation from the Changchun University of Technology, Changchun, China, in 2019 , where he is currently working toward M.S. degree at the Department of Mechanical Engineering. His research interests include triboelectric nanogenerators and piezoelectric actuators.

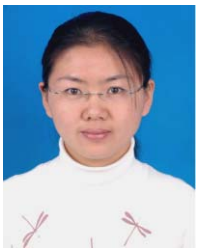

XIAOHUI LU was born in Jilin, China. She received the B.S. degree inmathematics and applied mathematics from Beihua University, Jilin, China, in 2004, the M.S. degree in operational research and cybernetics from the Lanzhou University of Technology, Lanzhou, China, in 2007, and the Ph.D. degree in control theory and application from Jilin University, Changchun, China, in 2013. She was a visiting scholar in School of College of Engineering at The Ohio State University under the supervision of Junmin Wang from 2017 to 2018. Her current research interests include vehicle powertrain control, model predictive control, data-driven control, and triboelectric nanogenerators.

This work is licensed under a Creative Commons Attribution 4.0 License. For more information, see https://creativecommons.org/licenses/by/4.0/